Journal of Probiotics & Health

OPEN ACCESS Freely available online

Research Article

Lactobacillus reuteri ATG-F4-Mediated Amelioration of Muscle Atrophy: Role of Gut Microbiota Composition and Short-Chain Fatty Acids

Daeyoung Lee*, Young-Sil Lee, Gun-Seok Park, Juyi Park, Seung-Hyun Ko, You-Kyung Lee, Do Yeun Jeong, Yong Hyun Lee, Jihee Kang

Department of Non-clinical Efficacy Assessment, AtoGen Company Research Institute, AtoGen. Co., Ltd., Daejeon, Republic of Korea

ABSTRACT

Probiotics offer a promising avenue for combating muscle atrophy, a debilitating condition associated with disuse, aging and disease. This study investigated the anti-atrophic potential of *Lactobacillus reuteri* ATG-F4, a human gut-derived bacterium, in a staple-induced immobilization mouse model. ATG-F4 administration significantly preserved muscle mass and improved grip strength and endurance, compared to disused controls. Mechanistically, ATG-F4 activated mammalian Target of Rapamycin (mTOR) signalling, promoting protein synthesis, while downregulating *MuRF1*, a key atrophy factor. Furthermore, ATG-F4 treatment demonstrably altered the gut microbiota composition, favoring the *Muribaculaceae* family and decreasing *Lachnospiraceae* and *Lactobacillaceae*. This regulation suggests that it may increase serum levels of the Short-Chain Fatty Acids (SCFAs) butyrate and acetate. These SCFAs are known to possess anti-inflammatory and muscle-beneficial properties. Therefore, this study suggests a novel mechanism for ATG-F4's anti-atrophic muscle: Enhancing muscle protein synthesis, suppressing protein degradation and modulating the gut microbiota-SCFA axis. These findings highlight the potential of ATG-F4 as a promising prophylactic or therapeutic agent for combating muscle atrophy.

Keywords: *Lactobacillus*, Probiotics, Muscle atrophy, Inflammation, Gut microbiota, Short-Chain Fatty Acids (SCFAs)

INTRODUCTION

Lactobacillus reuteri ATG-F4 is a strain isolated from neonatal feces. *Lactobacillus reuteri* has been shown to have various physiological activities, including: Improvement of Inflammatory Bowel Disease (IBD) symptoms, inhibition of Colorectal Cancer (CRC), immunomodulation [1-3]. In this study, we demonstrated that *Lactobacillus reuteri* ATG-F4 supplementation attenuates muscle atrophy. We found that this effect was mediated by an increase in Short-Chain Fatty Acids (SCFAs) and a decrease in inflammatory cytokines, which led to the inhibition of muscle atrophy signalling pathways. Furthermore, we observed changes in the gut microbiota composition following *Lactobacillus reuteri* ATG-F4 administration in a physical muscle atrophy model.

Probiotics are one of the fastest-growing categories with scientifically proven therapeutic evidence [4,5]. Some probiotic strains promote the health of your gut microbiome, which can help prevent some common diseases, such as obesity, diabetes, autism, osteoporosis and some immune disorders [6].

From another point of view, a number of research papers have been reported that probiotics can also affect each other in various organs such as the brain, liver, lungs, bones and muscles [7-11]. Since probiotics cannot act directly on organs other than the digestive system, the changes of metabolites or immune functions by probiotics may affect various organs. That is, the regulation of intestinal microbes using probiotics is important for improving organ function, which is emerging as an alternative to developing therapeutic agents.

Basically, skeletal muscle is an important tissue that moves the human body and has functions such as storing carbohydrates as an energy source and regulating body temperature. Meanwhile, muscle mass can be easily lose depending on nutritional status, hormonal balance, physical activity, injury, illness and aging. In particular, muscle atrophy occurs in diseases such as cancer, Acquired Immuno Deficiency Syndrome (AIDS), Duchenne Muscular Dystrophy (DMD), renal and heart failure, Chronic Obstructive Pulmonary Disease (COPD) and diabetes [12,13]. Muscle atrophy adversely affects the recovery and longevity and

Correspondence to: Daeyoung Lee, Department of Non-clinical Efficacy Assessment, AtoGen Company Research Institute, AtoGen. Co., Ltd., Daejeon, Republic of Korea, Email: d.lee@atogen.co.kr

Received: 22-Feb-2024, Manuscript No.JPH-24-30601; **Editor assigned:** 26-Feb-2024, Pre QC No. JPH-24-30601(PQ); **Reviewed:** 11-Mar-2024, QC No. JPH-24-30601; **Revised:** 18-Mar-2024, Manuscript No.JPH-24-30601(R); **Published:** 25-Mar-2024, DOI: 10.35248/2329-8901.24.12.349

Citation: Lee D, Lee YS, Park GS, Park J, Ko SH, Lee YK, et al. (2024) *Lactobacillus reuteri* ATG-F4-Mediated Amelioration of Muscle Atrophy: Role of Gut Microbiota Composition and Short-Chain Fatty Acids. J Prob Health. 12:349

deteriorates the quality of life, because muscle mass can influence general metabolism, locomotion and respiration [14]. Therefore, research and development for the prevention or treatment of muscle atrophy are one of the challenges to be solved for human health.

Research papers in associated with relationship between muscle and gut microbiota have been reported over the years [15,16]. Changes in gut microbiota by prebiotics increased muscle mass in obese and type 2 diabetic mice models [17]. *Akkermansia muciniphila* and *Faecalibacterium prausnitzii* strains inhibited muscle atrophy factor such as *Atrogin-1*, *MuRF1* and *Bifidobacterium breve* B-3 activated the mTOR-p70S6K signalling pathway in muscle [18,19]. These studies suggest a link between gut microbes and muscle metabolism.

In this study, we utilized the hind limb immobilization to induce a physical muscle atrophy of mice. There is currently no study investigating the effects of probiotics on gut microbiota and muscle function in a hind limb immobilization model. Since the hind limb immobilization is effective in reducing skeletal muscle mass and increasing intramuscular cytokines, it could affect the gut microbiota.

Intestinal dysbiosis affects local and systemic inflammation ofthe host and can affect metabolic diseases and specific organs.We hypothesized that intestinal dysbiosis may be associated with muscular atrophy and that disturbances in the intestinalmicrobiota and host relationship may exist. In the present study, we investigated the effects of *Lactobacillus reuteri* ATG-F4 on gut microbiota and muscle mass, using a staple-immobilization model.

MATERIALS AND METHODS

Lactobacilli strains

Lactobacillus reuteri ATG-F4 strain was isolated from newborn in the previous study [20]. ATG-F4 was cultured on de Man Rogosa Sharpe (MRS) medium (Difco Laboratories, USA) at 37°C for 24 h. The cultured ATG-F4 was centrifuged at 4,000 × g for 10 minutes to obtain only the cells, then washed two times by Phosphate-Buffered Saline (PBS) and diluted and then used for animal experiment.

Bioethics declaration

Ethics approval for animal study was provided by the Institutional Animal Care and Use Committee (IACUC) of AtoGen Co., Ltd., and the registration number is ATG-IACUC-RDSP-200713.

Study selection process

The title and summary of each of the studies that were identified by the search were evaluated by two reviewers (LDG and HAR); duplicate articles were discarded, as were those that did not meet the inclusion criteria.

Animals and experimental group

Five-week-old C57BL/6J male mice were purchased from central lab. Animal Inc. (Seoul, Korea). The facility was maintained at a temperature of 23 ± 2°C and a humidity of 55 ± 10%, with a 12-h light/dark cycle. Mice fed a normal diet (Cargill Inc, Purina® and Korea) and drank sterilized distilled water. Mice were randomly divided into three treatment groups: Untreated (n=10), stapled (n=10), stapled+ATG-F4 (n=10) after a 1-week acclimation period.

ATG-F4 was administered orally at a dose of approximately 4.0 × 10^9 Colony Forming Unit (CFU)/mice for a total of 27 days, while the untreated group and staple fixation group were administered PBS. On day 14 of the treatment, the right leg of each mouse in the staple fixation group was fixed with a staple for 10 days. Three days after staple removal, fresh fecal samples were collected from each mouse in an empty cage. Additionally, a wire hanging test and a treadmill test were performed on all animals to assess the improvements in muscle rehabilitation and exercise capacity due to ATG-F4 consumption.

All animals were sacrified the day after muscular performance test. Blood samples were collected after euthanasia by CO_2 inhalation and freshly obtained serum samples were processed for cytokines and metabolome analysis. Five types of leg skeletal muscle such as Tibialis Anterior (TA), Gastrocnemius (GA), Plantaris (PL), Extensor Digitorum Longus (EDL) and Soleus (SOL) were separated and their weights were compared. All muscle tissues were stocked in liquid nitrogen and moved to -70°C until they were analyzed.

Wire hang test

The wire hang test was performed using a 440 × 330 mm square of wire mesh consisting of 10 mm each in width and length per diameter wire [21]. The time was measured after the mouse was placed to the center of the wire screen and turned over. The screen was fixed at least 40 cm up above a padded surface to absorb the shock when it fell. All animals had warming-up for three minutes on the wire without a weight. The experiment was conducted by hanging a weight of approximately 25% of mice body weight and maximum time set 300 seconds. The wire hang test was repeated three times independently. Recording the falling time of the mouse was compared and analyzed by the average value. Furthermore, the falling time was re-evaluated as score following as; falling time between 1-60 seconds=1, falling time between 61-120 seconds=2, falling time between 121-180 seconds=3, falling time between 181-240 seconds=4, falling time between 241-300 seconds=5 and falling time after 300 seconds=6.

Treadmill test

The treadmill test was performed with reference to the protocol used for the running test using 5 lane treadmill for mice (Harvard Apparatus, USA) [22,23]. Before starting the experiment, the mice were warmed up at a speed of 8 m/min for five minutes.The starting point was 1.25 mA of electrical stimulation to induce mouse running. For the actual test, starting at a speed of 10 m/min, settings were made to automatically increase the speed by 2 m/min every 10 minutes. The running time was measured up to 80 minutes in eight steps. After half hour, the angle was started to increase to two degrees every 10 minutes, the angle was increased up to 10°. Despite the application of electrical stimulation, the experiment was terminated on assumption that the mice were exhausted when mice got electrical shock five times at one step. After the experiment was completed, the measured running time and distance of the mouse were recorded to analyze.

Cytokine assay

The levels of TNF-α and IL-6 in the serum and the supernatant of the crushed muscle tissues were measured using a commercial kit (mouse TNF-α and IL-6 Enzyme Linked Immuno Sorbent Assay (ELISA) max standard set, BioLegend). The values of TA and GA muscles were revised to the protein concentration measured by Bicinchoninic Acid (BCA) kit and expressed as pg/mg.

Western blot analysis

Flash-frozen TA and GA muscles were thoroughly crushed in liquid nitrogen. And Radio Immuno Precipitation Assay (RIPA) buffer (0.5 M Tris-HCl, pH 7.4, 1.5 M NaCl, 2.5% deoxycholic acid, 10% NP-40) containing a protease inhibitor cocktail (Millipore, USA) was added to the crushed muscle tissues after liquid nitrogen was evaporated. The homogenate was centrifuged at 14,000 rpm for 10 min at 4°C and the supernatant was recovered. Protein concentrations in the supernatant were determined using Bicinchoninic Acid Assay (BCA) assay (Thermo Fisher, USA). The protein extract (40 μg) was separated on 8% or 10% polyacrylamide mini gel and transferred to a Poly Vinylidene Fluoride membrane

(PVDF) that uses the most of (Bio-Rad, USA), blotted membranes were incubated overnight at 4°C in super block blacking buffer (pH 7.4) containing Kathon™, anti-microbial agent with anti-mTOR (1:1000; cell signalling), anti-p-mTOR (1:1000; cell signalling),anti-p70S6K (1:1000; cell signalling), anti-p-p70S6K (1:1000; cell signalling), anti-rpS6 (1:1000; cell signalling), anti-p-rpS6 (1:1000; cell signalling), anti-MURF1 (1:1000; Mybiosource), anti-atrogin-1 (1:1000; Mybiosource), beta actin (1:1000; cell signalling). The blots were washed four times with 0.1% tween Tris-Buffered Saline (TBS) before being incubated for 1 h at room temperature with goat anti- rabbit IgG Horseradish Peroxidase (HRP) conjugated secondary antibody (Bio-Rad, USA) in 0.1% tween TBS buffer containing 3% Bovine Serum Albumin (BSA) (Bovogen, USA). After extensivewashes with 0.1% tween TBS, the immuno stained bands were revealed with Enhanced Chemiluminescence (ECL) (Bio-Rad, USA). The target complex was detected by ChemiDoc™ Imaging System (Bio-Rad, USA). The target band intensity was quantified using the Image Lab™ software (Bio-Rad, USA).

Real-time polymerase chain reaction

Total Ribonucleic Acid (RNA) was extracted from flash-frozen TA and GA muscles using TRIzol (Thermo Fisher, USA) after crushed them in liquid nitrogen. The homogenate keeping on ice was added chloroform and centrifuged 13,000 g, 4°C for 5 min and the supernatant was recovered. Isopropanol which was set 70%of final concentration were added to get RNA precipitate fromthe homogenate by centrifugation (13,000 g, 4°C for 5 min) and this performance was repeated twice by 70% of ethanol. Diethyl Pyrocarbonate (DEPC) water was added to RNA precipitation after drying solvent at room temperature. Complementary Deoxy Ribonucleic Acid (cDNA) was synthesized from the 1 µg of RNA using AccPower RT PreMix (Bioneer, Korea). Primers for PCR amplification were as follows: *5'-ACACTGGTGCAGAGAGTCGG-3'* (forward) and *5'-TAAGCACACAGGCAGGT CGG-3'* (reverse) for *Atrogin-1* and *5'-GCGTGACCACAGAGGGTAAAGA-3'* (forward) and *5'-GTGGGGAGCCCTATGCTAGTC-3'* (reverse) for *MuRF1*. Beta actin (GenBank accession no. NM_007393) was amplified by PCR from AccuPower qPCR primer a set (Bioneer, Korea). The quantitative Reverse Transcription Polymerase Chain Reaction (RT-PCR) assays were performed using 10 ng of cDNA with power UPTM SYBRTM green master mix (Thermo Fisher Scientific, USA) and primers by 7500 fast real-time PCR System (Thermo Fisher Scientific, USA). Quantitative Polymerase Chain Reaction (qPCR) conditions for all reactions included an initial 20 seconds denaturation step at 95°C, followed by 45 cycling stages 3 seconds at 95°C and 30 seconds at 60°C.

Histology

TA and GA muscles were excised, fixed in 10% formalin for more than 48 h at room temperature. The fixed tissue was subjected to general tissue processing procedures such as trimming, dehydration, paraffin embedding and thinning, to prepare a specimen for histopathological examination and then staining Hematoxylin and Eosin (H and E). Histopathological changes were observed byH and E slide pictures which were taken a 400-fold enlargement using an optical microscope (Olympus BX53, Japan). Myofiber sizeresults are obtained from the Cross-Sectional Area (CSA) of H andE stain sections. Over 30 myofibers/field from 3 different views was examined.

Fecal microbiota analysis

Genomic DNA extraction from fecal samples was performed using the QIAamp Power Fecal Pro DNA Kit (Qiagen, Germany). The quantity and quality of extracted DNA were measured using Qubit 3.0 Fluorometer (Thermo Fisher Scientific, USA) and agarose gel electrophoresis, respectively. The V4 hypervariable regions of the bacterial 16S ribosomal RNA (rRNA) were amplified with unique 8 bp barcodes and sequenced on the Illumina iSeq 100 system plATGorm according to standard protocol [24]. The raw sequence data were submitted to the National Center for Biotechnology Information Sequence Read Archive (NCBI's SRA) database NCBI Bio project, raw data accession number: PRJNA694467. Raw reads were analyzed using the Quantitative Insights Into Microbial Ecology (QIIME2) pipeline [25]. Sequences were quality filtered and clustered into operational taxonomic units at 97% sequence identity according to the SILVA 132 database [26]. The operational taxonomy units were identified at phylum to family levels.

Short chain fatty acids analysis

Acetic acid (≥ 99.8% purity), butyric acid (≥ 99.5% purity) and propionic acid (≥ 99.5% purity) were of analytical grade purchased from Sigma-Aldrich (St. Louis, MO, USA). Ammonium formate (≥ 99.995% purity), formic acid (≥ 99.5% purity), High-Performance Liquid Chromatography (HPLC) grade Methanol (MeOH), HPLC grade Acetonitrile (ACN) and HPLC grade water were purchased from Sigma-Aldrich. A 100 µL aliquot of serum was mixed with 500 µL of ice-cold MeOH with 1% formic acid. The solution was mixed by vortex for 20 minutes and left for 2 hours (4°C) to solidify the protein precipitate. After centrifugation at 14,000 rpm for 30 min at 4°C, the supernatant was filtrated by using a Poly Vinylidene Fluoride (PVDF) syringe filter (0.22 µm pore size) (Millipore, Billerica, MA). The filtrated sample was injected into the Liquid Chromatography-tandem Mass Spectrometry (LC-MS/MS) system. LC-MS/MS analyses were carried out using an exion LC system connected to a QTRAP 4500 mass spectrometer (AB SCIEX, Framingham, MA, USA). The LC analyses were carried out using an intrada organic acid column (150 × 2 mm, 3-µm particle size, Imtakt Kyoto, JPN). A 5 µL aliquot was used forthe auto sampler injection and the flow rate was 0.2 mL/min at 40°C. The negative ion mode scanning of a gradient mobile phase,consisting of (A) acetonitrile/water/formic acid (10/90/0.1, v/v) solution and (B) acetonitrile/100 mM ammonium formate (10/90,v/v) solution, was used. The gradient started at 0% B and was heldat this value for 1 min. The gradient increased linearly to 100% B in 6 min. The mobile phase composition was held at 100% B for3 min before it returned to 0% B in 0.1 min. Finally, the gradientwas kept at 0% B for 4.9 min to re-equilibrate the column. The total analysis time was 15 min. The analysis was performed using an electrospray ionization source in negative mode. The operationconditions were as follows: Ion spray voltage, 4500 V; Curtaingas (CUR), 25 psi; Collisionally Activated Dissociation (CAD), medium; ion Source Gas 1 (GS 1) and ion Source Gas 2 (GS 2), 50and 50 psi; the turbo spray temperature 450°C; Entrance Potential(EP), 10 V; Collision cell Exit Potential (CXP), 5 V. Nitrogen was used in all cases. Analytes were quantificated by Multiple Reaction Monitoring (MRM) employing the following precursor to product ion transitions and parameters: Acetic acid, m/z 105.0 → 44.9 withDP 5 V and CE 18 eV; butyric acid, m/z 133.0 → 44.9 with DP 5 Vand CE 18 eV; propionic acid, m/z 119.0 → 45.1 with DP 5 V andCE 16 eV. SCIEX OS 2.0.0 software was used for data acquisition and processing and analyst 3.3 software was used for data analysis.

Statistical analyses

All data are expressed as means ± Standard Error of Mean (SEM). One-way Analysis of Variance (ANOVA) with Dunnett's test was used for multiple comparison by graph pad prism 8.0 software. Differences were considered statistically significant at $P<0.05$. For the fecal microbiota analysis, the non-parametric kruskal-wallistest was used to compare the differences in diversity indexes and micro bial taxa.

RESULTS

Effects of *L. reuteri* ATG-F4 on body weight and muscles weight

The total body weights among all three groups showed no significant differences after 10 days of immobilization and three days of staple removal (Figure 1A). However, the muscle mass of TA, GA, PL, EDL and SOL in the stapled group was atrophied by 28.9%, 30.3%, 28.0%, 20.7% and 15.3%, respectively, compared to the untreated group. Treatment with ATG-F4 resulted in a significant form of increase in muscle mass of TA, GA and PL by 17.3%, 30.3% and

27.0%, respectively, compared to the stapled group (Figures 1B-1G). Additionally, the total muscle mass of the hind limb was significantly augmented by 22.4% with ATG-F4 compared to the stapled group (Figure 1H).

Effects of *L. reuteri* ATG-F4 on myofiber size

We analyzed the Cross-Sectional Area (CSA) of myofibers in the TA and GA muscles of each experimental group, following H and E staining. The average size of myofibers in the TA and GA muscles of the stapled group was decreased compared to the untreated group, while the size of myofibers in both TA and GA muscles of the ATG-F4 group was significantly increased compared to the stapled group (Figures 2A-2C). Moreover, there was a significant increase in the percentage of large myofibers in the TA and GA muscles of the ATG-F4 group compared to the stapled group (Figures 2D and 2E).

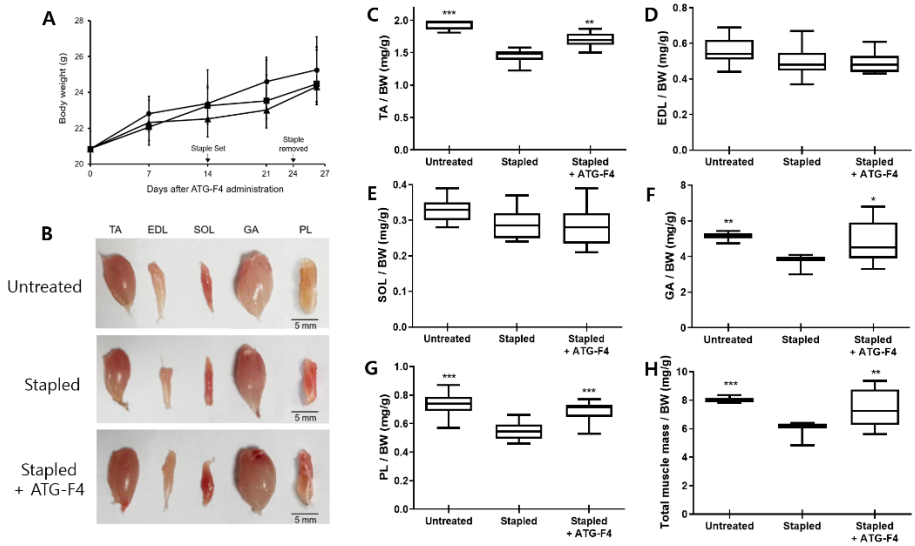

Figure 1: Changes of bodyweight and muscle mass of hind limb. (A): Bodyweight; (B): Pictures of hind limb; (C-H): Relative weight of TA (C), EDL (D), SOL (H), GA (F), PL (G) and Total muscle (H); **Note:** TA: Tibialis Anterior; EDL: Extensor Digitorum Longus; SOL: Soleus; GA: Gastrocnemius; PL: Plantaris. Untreated: Unstapled group; Stapled: Hind limb immobilization group; Stapled+ATG-F4: Hind limb immobilization+*L. reuteri* ATG-F4 (4.0×10^9 CFU/day) treated group. Data are presented as means ± SEM; (*): p<0.05; (**): p<0.01 and (***): p<0.001 compared to stapled. (●):Unstapled; (■):Stapled; (▲): Stapled+ATG-F4.

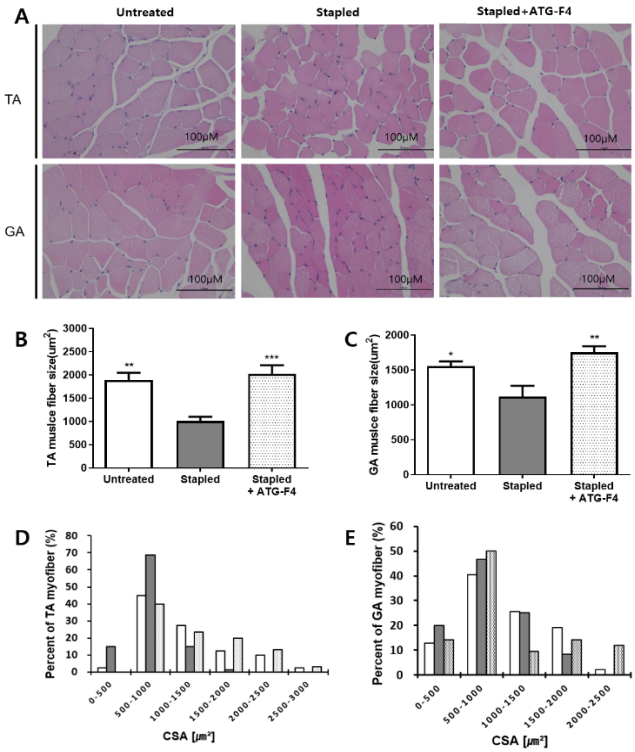

Figure 2: H and E staining of TA and GA muscle fibers. (A): Representative pictures of TA and GA muscle fiber; (B-C): Quantification of Cross-Sectional Area (CSA) in TA (B) and GA (C) Muscle fibers; (D-E): Myofiber size distribution of TA and GA Muscle. Note: TA: Tibialis Anterior; GA: Gastrocnemius; Untreated: Unstapled group; Stapled: Hind limb immobilization group; Stapled+ATG-F4: Hind limb immobilization+*L. reuteri* ATG-F4 (4.0×10^9 CFU/day) treated group. Data are presented as means ± SEM; (*): p<0.05; (**): p<0.01 and (***): p<0.001 compared to stapled. (□): Untreated; (■): Stapled; (▣): Stapled+ATG-F4.

Effects of *L. reuteri* ATG-F4 on muscle function

To estimate muscle strength, we performed the wire hang test 3 days after staple removal, with timing beginning as soon as a mouse faced down on the wire. The latency to fall and average maximum score of ATG-F4-treated mice were significantly higher than those of the stapled group, at 188.9 ± 80.2 *vs.* 116.1 ± 29.2 and 4.0 ± 1.7 *vs.* 2.7 ± 0.7, respectively (Figures 3A and 3B). In the treadmill test to assess muscle functional recovery, the running time to exhaustion for the stapled group mice was significantly shorter than that for the untreated group. In contrast, the ATG-F4 group showed a significant increase in both running time and distance compared to the stapled group, at 48.7 ± 14.2 *vs.* 34.9 ± 11.2 and 716.6 ± 294.5 *vs.* 445.9 ± 182.1, respectively (Figures 3C and 3D).

Effects of *L. reuteri* ATG-F4 on cytokines levels in serum and muscle tissues

The levels of inflammatory cytokines were measured in the serum, TA and GA muscles. Tumor Necrosis Factor-alpha (TNF-α) and Interleukin-6 (IL-6) levels were increased in the serum and muscle tissues of the stapled group compared to the untreated group. Treatment with ATG-F4 resulted in reduced levels of TNF-α in the serum and TA muscle compared to the stapled group (Figures 4A and 4B). The level of IL-6 in the serum of the ATG-F4 group was significantly lower than the stap led group (Figures 4C and4D). Moreover, ATG-F4 treatment also decreased the level of IL-6 in TA and GA muscles (Figures 4E and 4F).

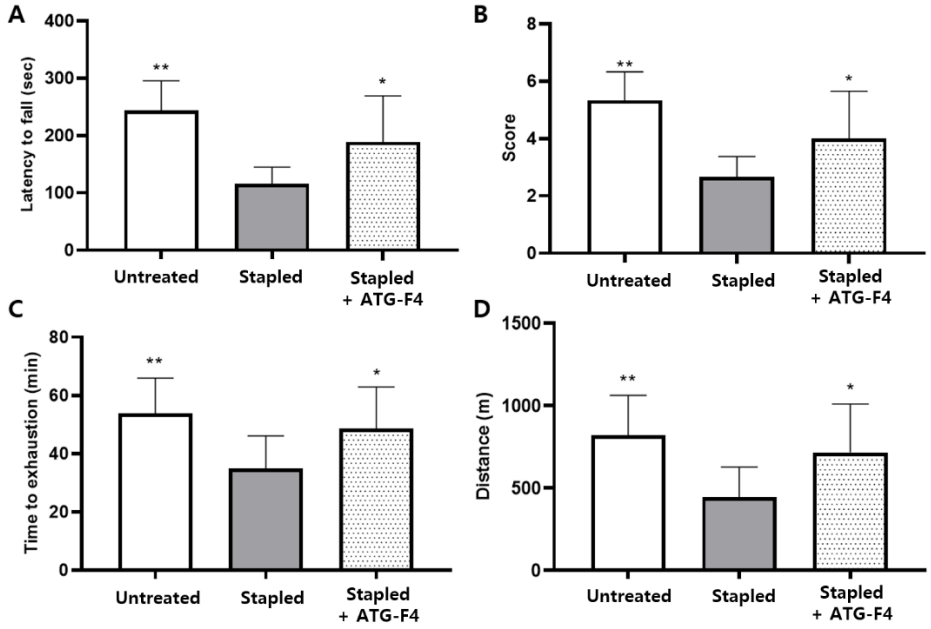

Figure 3: Physical performance of muscle strength and endurance. (A, B): Latency to fall (A) and its score (B) in wire hang test for muscle strength;(C, D): Running time to exhaustion (C) and its distance (D) in treadmill test; Untreated: Unstapled group; Stapled: Hind limb immobilization group; Stapled+ATG-F4: Hind limb immobilization+*L. reuteri* ATG-F4 (4.0×10^9 CFU/day) treated group. Data are presented as means ± SEM; (*): p<0.05; (*): p<0.01 and (**): p<0.001 compared to Stapled.

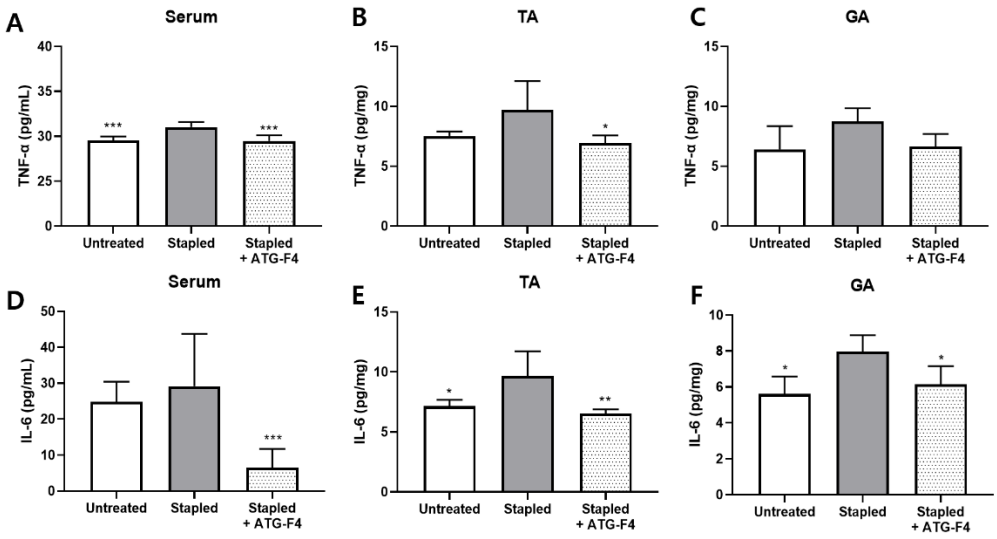

Figure 4: Levels of inflammatory cytokine the serum and muscle tissues. (A-C): The level of Tumor Necrosis Factor alpha (TNF-α) in serum (A), TA (B), GA (C) muscle; (D-F): The level of Interleukin (IL-6) in serum (D), TA (E), GA (F) muscle of the level of IL-6. **Note:** TA: Tibialis Anterior; GA: Gastrocnemius; Untreated: Unstapled group; Stapled: Hind limb immobilization group; Stapled+ATG-F4: Hind limb immobilization+*L. reuteri* ATG-F4 (4.0×10^9 CFU/day) treated group. Data are presented as means ± SEM; (*): p<0.05; (**): p<0.01 and (***): p<0.001 compared to stapled.

Effects of *L. reuteri* ATG-F4 on the expression of muscle atrophy related genes and proteins

The messenger Ribonucleic Acid (mRNA) and protein expression levels of muscle atrophy-related factors such as *Atrogin-1* and *MuRF1* in the TA and GA muscles were investigated using Reverse Transcription-quantitative Polymerase Chain Reaction (RT-qPCR) and western blot analysis, respectively. In the TA muscle, the expression levels of *Atrogin-1* in the stapled group weredecreased compared to the untreated group. However, there was nosignificant difference in the expression level of *Atrogin-1* between the ATG-F4 and stapled groups (Figures 5A and 5B). The expression levels of *MuRF1* in the stapled group were not decreased comparedto the untreated group, but the expression level of *MuRF1* was significantly decreased in the ATG-F4 group compared to the stapled group (Figures 5C and 5D). In the GA muscle, the expression levels of *Atrogin-1* and *MuRF1*in the stapled group were not significantly different from the untreated group (Figures 5E and 5F). The expression level of *Atrogin-1*was not significantly different between the ATG-F4 and stapled groups, however, the expression level of MuRF1 was significantly decreased in the ATG-F4 group compared to the stapled group (Figures 5G and 5H).

Effects of *L. reuteri* ATG-F4 on the phosphorylation of proteins related to muscle synthesis in muscle

We investigated the effects of ATG-F4 treatment on the phosphorylation of muscle synthesis-related proteins in TA and GA muscles using the western blotting method. The phosphorylation levels of muscle synthesis-related factors such as mTOR, P70S6K, rpS6 and 4E-BP1 in the TA muscle of the stapled group were not significantly different from those of the untreated group. However, the relative phosphorylation of these proteins in the TA muscle was significantly increased by ATG-F4 treatment (Figures 6A-6F). In the GA muscle, the expression levels of muscle synthesis-relatedfactors in the stapled group were either not different or decreased compared to the untreated group. As with the TA muscle, the relative phosphorylation of muscle synthesis factors in the GA muscle was also increased by ATG-F4 treatment (Figures 6G-6J).

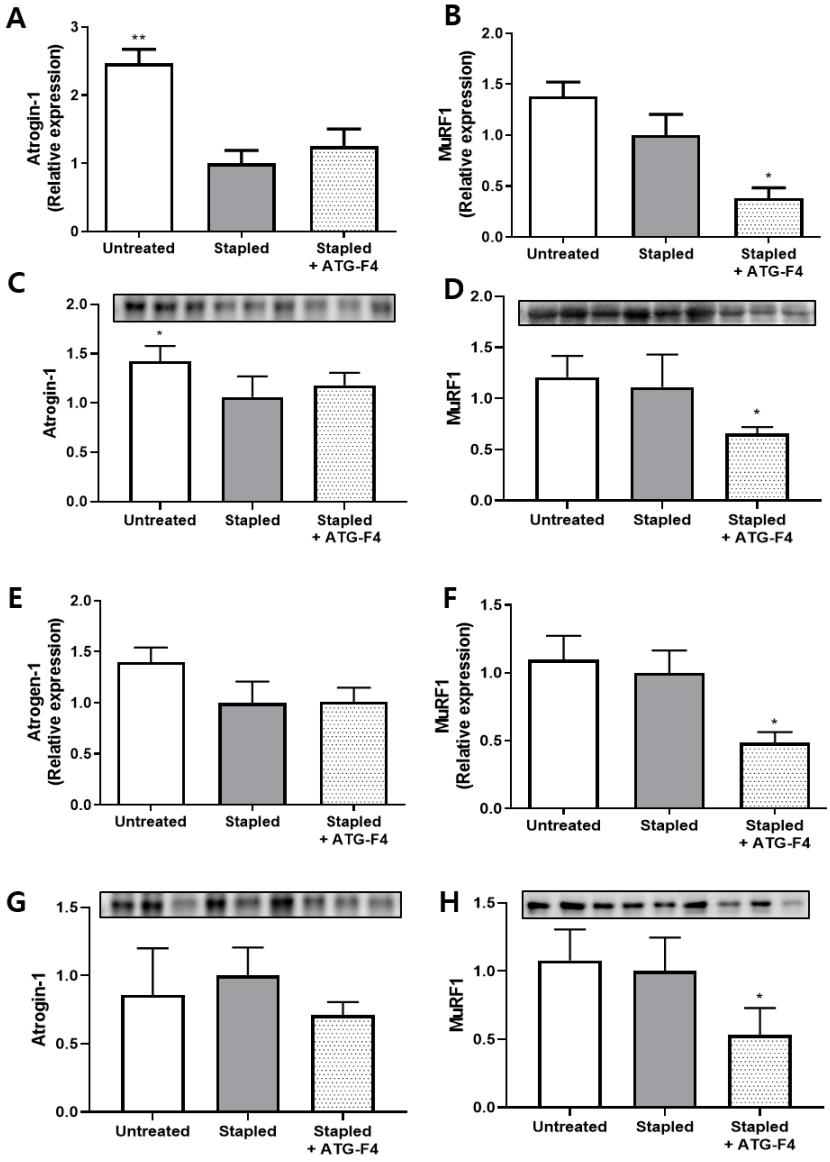

Figure 5: Expression of muscle atrophy factors in muscles. (A, B): The messenger Ribonucleic Acid (mRNA) expression of Atrogin-1 (A) and MuRF1 (B) in TA muscle; (C, D): The protein expression of Atrogin-1 (C) and MuRF1 (D) in TA muscle; (E, F): The mRNA expression of Atrogin-1 (E) and MuRF1 (F) in GA muscle; (G, H): The protein expression of Atrogin-1 (G) and MuRF1 (H) in GA muscle. **Note:** TA: Tibialis Anterior; GA: Gastrocnemius; Untreated: Unstapled group; Stapled: Hind limb immobilization group; Stapled+ATG- F4: Hind limb immobilization+*L. reuteri* ATG-F4 (4.0×10^9 CFU/day) treated group. Data are presented as means ± SEM; (*): $p<0.05$; (**): $p<0.01$ compared to stapled.

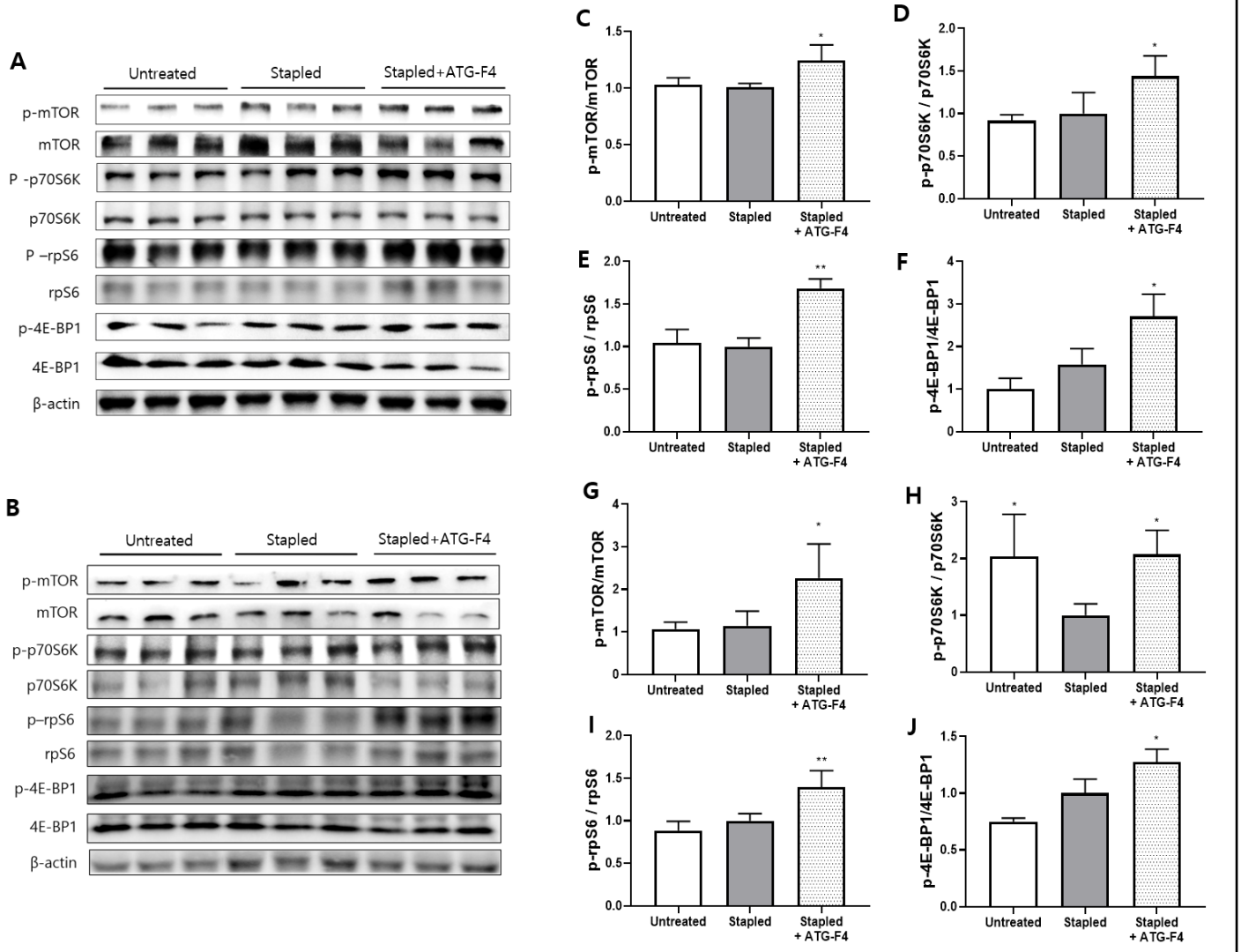

Figure 6: Phosphorylation of muscle synthesis proteins in muscles. (A, B): Representative immunoblotting of the muscle synthesis proteins TA (A)and GA (B), respectively; (C-F): Relative phosphorylation levels (or expression levels) of mTOR (C) and p70S6K (D), rpS6 (E), 4E-BP1 (F) in TA muscle; (G-J): Relative phosphorylation levels (or expression levels) of mammalian Target of Rapamycin mTOR (G) and p70 ribosomal S6 kinase p70S6K (H), ribosomal protein S6 rpS6 (I), 4E-BP1 (J) in GA muscle; **Note:** TA: Tibialis Anterior; GA: Gastrocnemius; Untreated: Unstapled group; Stapled: Hind limb immobilization group; Stapled+ATG-F4: Hind limb immobilization+*L. reuteri* ATG-F4 (4.0×10^9 CFU/day) treated group. Data are presented as means ± SEM; (*): $p<0.05$; (**): $p<0.01$ compared to stapled.

Fecal bacterial community analysis

The changes in gut microbial community were investigated by analyzing fecal samples from each experimental group. Taxonomic abundance analysis revealed a significant increase in the population of *Bacteroidetes* and a significant decrease in the population of *Firmicutes* in the ATG-F4 treated group. At the family level, the relative abundance of *Muribaculaceae* (phylum *Bacteroidetes*) showed a significant increase (Figures 7A and 7B), while the relative of abundance *of Lachnospiraceae* (phylum *Firmicutes*) and *Lactobacillaceae* (phylum *Firmicutes*) showed the significant decrease in the ATG-F4 group, similar to the untreated group (Figures 7C and 7D).

Metabolome analysis

The gut microbiome-related metabolites, Short-Chain Fatty Acids (SCFAs), were analyzed in serum using LC-MS/MS. Thelevel of butyric acid was increased in the stapled group compared to the untreated group and the ATG-F4 group showed a greater increase than the stapled group (Figure 8A). The level of acetic acidwas not significantly different between the untreated and stapled groups, but the ATG-F4 group showed a higher level of acetic acidthan the stapled group (Figure 8B). The levels of propionic acid did not show significant differences among all groups (Figure 8C).

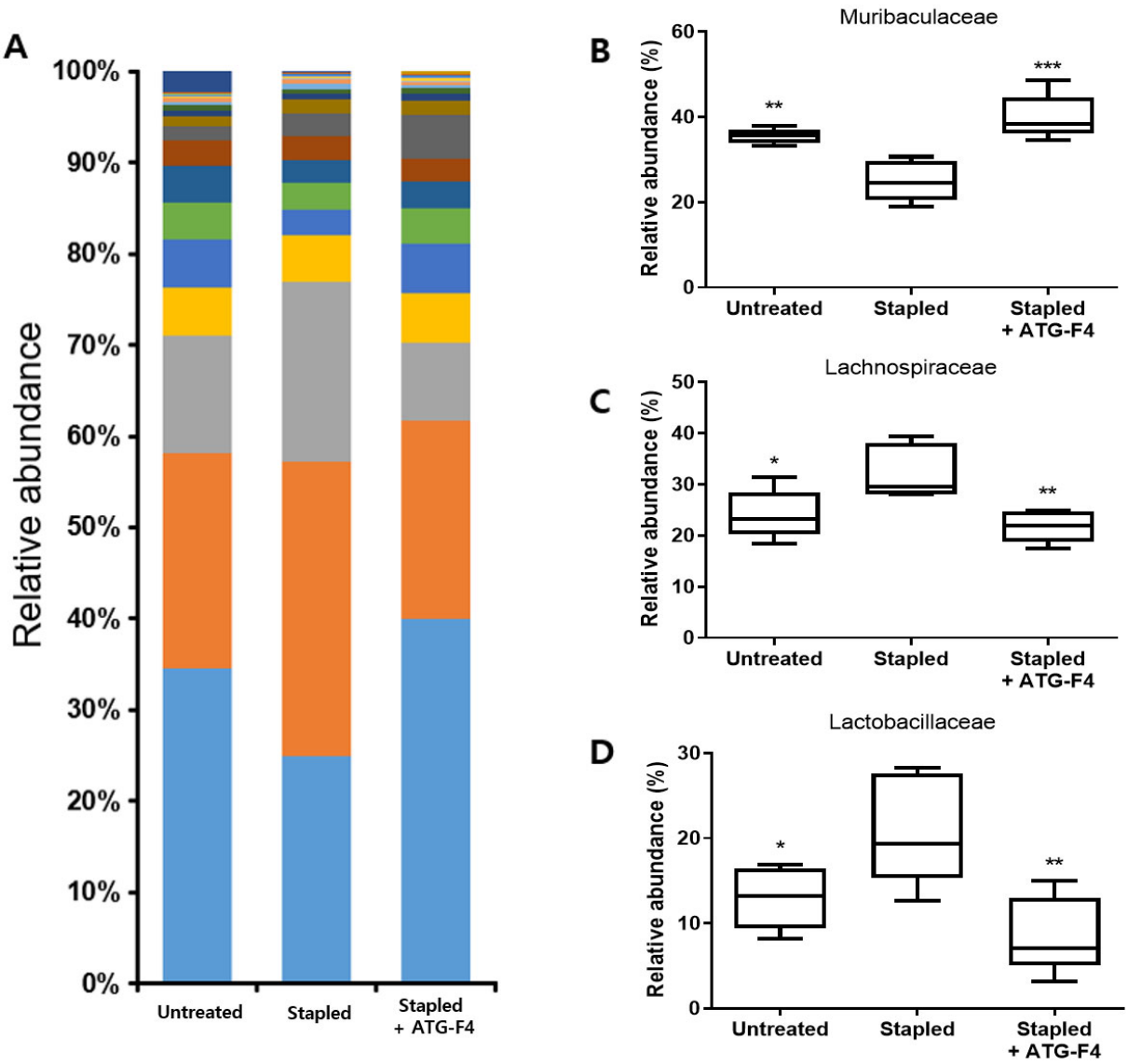

Figure 7: Changes in fecal bacterial community. (A): Stacked bar plot of top 17 abundant family level taxa; (B-D): Relative abundance of *Muribaculaceae* (B), *Lachonospiraceae* (C), *Lactobacillaceae* (D). **Note:** Untreated: Unstapled group; Stapled: Hind limb immobilization group; Stapled+ATG-F4: Hind limb immobilization + *L. reuteri* ATG-F4 (4.0×10^9 CFU/day) treated group. (*): $p<0.05$; (**): $p<0.01$ compared to stapled, (■): Family XIII; (■): *Burkholderiaceae*; (■): *Deferribacteraceae*; (■): Clostridiales vadinBB60 group; (■): *Desulfovibrionaceae*; (■): *Tannerellaceae*; (■): *Eggerthellaceae*; (■): *Clostridiaceae 1*; (■): *Erysipelotrichaceae*; (■): N/A; (■): *Rikenellaceae*; (■): *Bacteroidaceae*; (■): *Prevotellaceae*; (■): *Ruminococcaceae*; (■): *Lactobacillaceae*; (■): *Lachnospiraceae*; (■): *Muribaculaceae*.

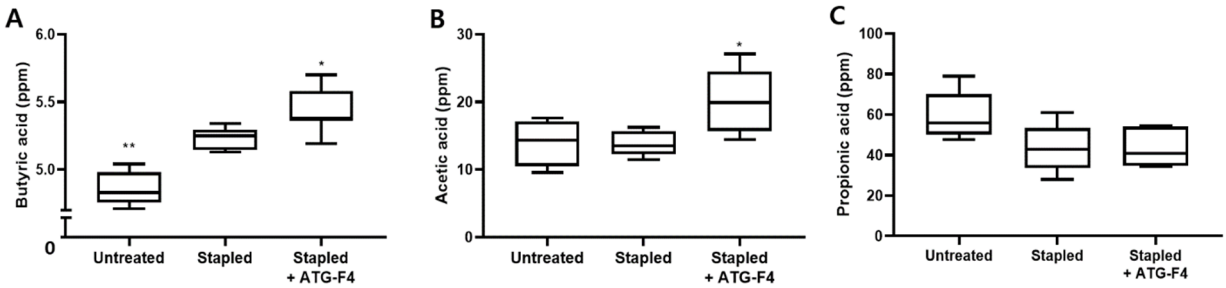

Figure 8: Changes of Short-Chain Fatty Acids (SCFAs) in serum. (A): Butyric acid; (B): Acetic acid; (C): Propionic acid. **Note:** Untreated: Unstapled group; Stapled: Hind limb immobilization group; Stapled+ATG-F4: Hind limb immobilization+*L. reuteri* ATG-F4 (4.0×10^9 CFU/day) treated group. Data are presented as means ± Standard Error of Mean (SEM); (*): $p<0.05$; (**): $p<0.01$ compared to stapled.

DISCUSSION

The present study aimed to investigate the potential of *Lactobacillus reuteri* ATG-F4 to ameliorate muscle atrophy and dysfunction. Additionally, we sought to elucidate the underlying mechanism of action in mice with muscle atrophy induced by staple immobilization. Our findings demonstrate that *Lactobacillus reuteri* ATG-F4 increased muscle mass and improved grip strength and endurance.

Moreover, the probiotic was found to suppress inflammation induced by disuse of muscle, indicating its potential to prevent or delay muscle loss. Based on these results, our study suggests that *Lactobacillus reuteri* ATG-F4 may be a promising candidate for preventing or delaying muscle atrophy by regulating inflammation and improving muscle function.

Increased inflammation levels in inactive muscles are thoughtto play a significant role in inducing muscle atrophy [27]. The regulation of muscle mass is a complex interplay between catabolic and anabolic processes, where downstream effectors of mTOR, including ribosomal protein (rpS6) and eIF4E-Binding Protein (4E-BP1), contribute to protein synthesis and muscle hypertrophy, while muscle atrophy-related genes *MuRF1* and *Atrogin-1* are responsible for protein breakdown and muscle wasting. It has been suggested that these two pathways are influenced by cytokines and modulated by the presence of inflammation [28-30]. Additionally, muscle fiber size is an important metric in determining muscle mass and strength, critical for assessing the extent of muscle loss [31-34].

In the previous experiment, no increase in muscle mass was observed in normal animals after 15 days of *L. reuteri* ATG-F4 administration. Similarly, it is speculated that *L. reuteri* ATG-F4 administration for 2 weeks before staple treatment in the current experiment did not affect muscle mass itself. Moreover, there was no significant difference in muscle recovery between four and seven days after staple removal with *L. reuteri* ATG-F4 administration. Thus, it is expected that *L. reuteri* ATG-F4 may have suppressed muscle atrophy during the staple period.

In this study, *L. reuteri* ATG-F4 was analyzed in samples dissected on the fourth day after staple removal. The results showed that *L. reuteri* ATG-F4 increased muscle fiber size, improved muscle function and decreased inflammation levels. The increase in muscle fiber size by *L. reuteri* ATG-F4 strongly supports muscle mass and strength gains [35]. On the other hand, while ATG-F4 increased treadmill endurance, there was no change in soleus muscle mass related to endurance. The increase in endurance due to the administration of *L. reuteri* ATG-F4 is expected to be associated with the increase in blood levels of BA and AA [36,37].

The results also showed that *L. reuteri* ATG-F4 increases phosphorylation of signalling pathway associated with mTOR in muscles and decreases the expression levels of *MuRF1*. On the other hand, no significant differences were observed in signalling pathway related to muscle synthesis and atrophy between the untreated group and the stapled group. Several papers have shown that signalling pathway related to muscle mass may increase or decrease during treadmill exercise depending on the experimental conditions [38-42]. Studies conducted under experimental conditions similar to the present study, including treadmill exercise and time of dissection, have reported an increase in *MuRF1* and mTOR associated with muscle atrophy after treadmill exercise [43,44]. Therefore, signalling pathway related to muscle atrophy and synthesis after treadmill exercise were increased in both the untreated and stapled group, suggesting that there may be no difference between the two groups. Nevertheless, it is interesting to note that ATG-F4, unlike the other groups, had a positive effecton muscle mass gain associated with muscle atrophy and synthesis.

The imbalance of microbial communities in the gut can cause intestinal barrier function, host metabolism and signalling pathways to be remodelled. These changes can be directly or indirectly related to gut dysbiosis and inflammation [45,46]. In addition, inflammation occurring within the body, such as that caused by lung or breast cancer, can lead to changes in gut microbiota [47]. It is believed that changes in gut microbiota in the staple immobilization model occur because inflammation originating from the muscles may have affected the gut.

Administration of *L. reuteri* ATG-F4 resulted in changes in gut microbiota; however, the *Lactobacillus* cluster did not increase with ATG-F4 administration. Treatment with *L. reuteri* ATG-F4 led to an increase in *Muribaculaceae* and a decrease in *Lachnospiraceae* and *Lactobacillaceae*, which tended to match the normal control group without stapled.

The abundance of *Muribaculaceae* is mostly decreased in many inflammation-related diseases [48-50]. However, *Lachnospiraceae* and *Lactobacillaceae* have been reported to increase or decrease depending on the inflammation model [48,51-53]. Regarding changes in microbial balance within the gut, more studies are needed to investigate whether *L. reuteri* ATG-F4 can alter the composition ratio of *Muribaculaceae*, *Lachnospiraceae* and *Lactobacillaceae*. However, it is noteworthy that *L. reuteri* ATG-F4 induced changes in the gut microbiota composition similar to those observed in healthy animals. Therefore, administering *L. reuteri* ATG-F4 could be a potential probiotic for improving gut microbiota imbalance.

The previously mentioned *Muribaculaceae*, *Lachnospiraceae* and *Lactobacillaceae* are dominant strains that account for approximately 70% of the total gut microbiota. These strains have the ability to ferment complex carbohydrates and dietary fiber, which leads to the production of Short-Chain Fatty Acids (SCFAs) as a byproduct [54]. SCFAs are essential for maintaining gut function, as they serve as an energy source for colon cells, reduce inflammationand improve intestinal motility [55-57]. Additionally, evidence is increasingly accumulating to suggest that SCFAs have beneficial effects on skeletal muscle metabolism and function [16,58].

BA, one of the SCFAs, has been reported to have anti-inflammatory properties and may act as an energy source for muscle [59-61]. It has also been reported that administration of BA to an aged rat model increases muscle mass and fiber size and the mechanism underlying the positive effects on muscle involves increased mTOR and inhibition of *MuRF1* [62,63]. In addition, AA may benefit muscle function by improving glycogen replenishment and increasing acetyl-CoA concentrations in skeletal muscle [64,65]. Due to the effects mentioned above, BA and AA are considered attractive SCFA metabolites for inhibiting muscle atrophy and increasing endurance [66].

The increase in blood concentrations of BA and AA following *L. reuteri* ATG-F4 administration suggests that *L. reuteri* ATG-F4 may stimulate the growth and activity of indigenous bacteria. These findings suggest that *L. reuteri* ATG-F4 can increase muscle mass in atrophied muscles, which may be accompanied by BA-induced upregulated mTOR and downregulated *MuRF1* pathways and the increase in AA may have contributed to the improvement of muscle endurance. However, unlike the similar bacterial community ratios observed in Normal Control (NC) and *L. reuteri* ATG-F4,BA and AA in serum were increased only in *L. reuteri* ATG-F4. Comparing the relative abundance of bacterial communities at the genus level with the concentration Increase/decrease pattern of BA and AA, a similar pattern was observed with *Parasutterella, Monoglobus, Faecalibaculum*. However, since these strains have a very low relative proportion, further experiments are needed to discuss the increase of BA and AA by ATG-F4 administration.

Many studies have shown that whole body inflammation interacts with the gut and that gut immune function can modulate whole body inflammation [67]. In addition, gut-derived substances produced in the gut can be transported throughout the body and exert various functions. As discussed above, *L. reuteri* ATG-F4 appears to improve muscle mass and function by restoring gut microbial communities, increasing serum BA and AA levels and suppressing inflammation. Based on our findings, *L. reuteri* ATG-F4 may regulate the gut microbiota-SCFAs (BA, AA)-muscle axis, thereby ameliorating muscle atrophy.

CONCLUSION

In this study, ATG-F4 was found to significantly increase muscle mass and fiber size, while improving muscle strength and exercise performance in a model of immobilized muscle atrophy. Concerning that probiotics are not absorbed into the body, but act within the digestive tract, ATG-F4, which regulates the gut microbiota and induces metabolomic changes in BA and AA, appears to have sufficient systemic effects. Through these actions, ATG-F4 was shown to reduce inflammatory cytokines in the blood, activate mTOR and inhibit *MuRF1* in the muscle, thereby inhibiting muscle atrophy. These results suggest that ATG-F4 has potential as a preventative or therapeutic agent for muscle atrophy. Furthermore, this research highlights the intriguing possibility of manipulating gut bacteria to combat muscle loss, opening new avenues for the development of novel therapeutic strategies for various conditions associated with muscle atrophy.

ACKNOWLEDGMENT

The present study was financially supported by Ministry of SMEs and Start-ups (grant no. S2912175; Development of functional health food materials to prevent sarcopenia using probiotics). We gratefully acknowledge the assistance of MSS.

AUTHOR CONTRIBUTIONS

DYL designed and conducted animal experiments and analysed data and wrote the manuscript. YSL carried out the animal experiment and edited the manuscript. GSP and SHK analyzed meta-analyses data of fecal microbiota and participated in manuscript writing. JY L and YK L participated in analysis of SCFAs. DYJ and YHL gave appropriate advices from preliminary data of staple model. JHK: Supervised the manuscript. All co-authors contributed to the manuscript and have approved the final manuscript.

REFERENCES

1. Wang H, Zhou C, Huang J, Kuai X, Shao X. The potential therapeutic role of *Lactobacillus reuteri* for treatment of inflammatory bowel disease. Am J Transl Res. 2020;12(5):1569.
2. Bell HN, Rebernick RJ, Goyert J, Singhal R, Kuljanin M, Kerk SA, et al. Reuterin in the healthy gut microbiome suppresses colorectal cancer growth through altering redox balance. Cancer Cell. 2022;40(2):185-200.
3. Luo Z, Chen A, Xie A, Liu X, Yu R. *Limosilactobacillus reuteri* in immunomodulation: Molecular mechanisms and potential applications. Front Immunol. 2023;14:1228754.
4. Stavropoulou E, Bezirtzoglou E. Probiotics in medicine: A long debate. Front Immunol. 2020;11:554558.
5. Novik G, Savich V. Beneficial microbiota. Probiotics and pharmaceutical products in functional nutrition and medicine. Microbes Infect. 2020;22(1):8-18.
6. Ranjha MM, Shafique B, Batool M, Kowalczewski PL, Shehzad Q, Usman M, et al. Nutritional and health potential of probiotics: A review. Appl Sci. 2021;11(23):11204.
7. Westfall S, Lomis N, Kahouli I, Dia SY, Singh SP, Prakash S. Microbiome, probiotics and neurodegenerative diseases: Deciphering the gut brain axis. Cell Mol Life Sci. 2017;74(20):3769-3787.
8. Cesaro C, Tiso A, Del Prete A, Cariello R, Tuccillo C, Cotticelli G, et al. Gut microbiota and probiotics in chronic liver diseases. Dig Liver Dis. 2011;43(6):431-438.
9. Forsythe P. Probiotics and lung diseases. Chest. 2011;139(4):901-908.
10. Amin N, Boccardi V, Taghizadeh M, Jafarnejad S. Probiotics and bone disorders: The role of RANKL/RANK/OPG pathway. Aging Clin Exp Res. 2020;32(3):363-371.
11. Jager R, Shields KA, Lowery RP, de Souza EO, Partl JM, Hollmer C, et al. Probiotic *Bacillus coagulans* GBI-30, 6086 reduces exercise-induced muscle damage and increases recovery. Peer J. 2016;4:e2276.
12. Dutt V, Gupta S, Dabur R, Injeti E, Mittal A. Skeletal muscle atrophy: Potential therapeutic agents and their mechanisms of action. Pharmacol Res. 2015;99:86-100.
13. Perry BD, Caldow MK, Brennan-Speranza TC, Sbaraglia M, Jerums G, Garnham A, et al. Muscle atrophy in patients with Type 2 diabetes mellitus: Roles of inflammatory pathways, physical activity and exercise. Exerc Immunol Rev. 2016;22:94.
14. Vinciguerra M, Musaro A, Rosenthal N. Regulation of muscle atrophy in aging and disease. Adv Exp Med Biol. 2010:211-233.
15. Liao X, Wu M, Hao Y, Deng H. Exploring the preventive effect and mechanism of senile sarcopenia based on "gut–muscle axis". Front Bioeng Biotechnol. 2020;8:590869.
16. Lustgarten MS. The role of the gut microbiome on skeletal muscle mass and physical function: 2019 update. Front Physiol. 2019;10:500047.
17. Everard A, Lazarevic V, Derrien M, Girard M, Muccioli GG, Neyrinck AM, et al. Responses of gut microbiota and glucose and lipid metabolism to prebiotics in genetic obese and diet-induced leptin-resistant mice. Diabetes. 2011;60(11):2775-2786.
18. Byeon HR, Jang SY, Lee Y, Kim D, Hong MG, Lee D, et al. New strains of *Akkermansia muciniphila* and *Faecalibacterium prausnitzii* are effective for improving the muscle strength of mice with immobilization-induced muscular atrophy. J Med Food. 2022;25(6):565-575.
19. Toda K, Yamauchi Y, Tanaka A, Kuhara T, Odamaki T, Yoshimoto S, et al. Heat-killed *Bifidobacterium breve* B-3 enhances muscle functions: Possible involvement of increases in muscle mass and mitochondrial biogenesis. Nutrients. 2020;12(1):219.
20. Beck BR, Park GS, Jeong DY, Lee YH, Im S, Song WH, et al. Multidisciplinary and comparative investigations of potential psychobiotic effects of *Lactobacillus* strains isolated from newborns and their impact on gut microbiota and ileal transcriptome in a healthy murine model. Front Cell Infect Microbiol. 2019;9:269.
21. Deacon RM. Measuring the strength of mice. J Vis Exp. 2013;(76):e2610.
22. Lagouge M, Argmann C, Gerhart-Hines Z, Meziane H, Lerin C, Daussin F, et al. Resveratrol improves mitochondrial function and protects against metabolic disease by activating SIRT1 and PGC-1α. Cell. 2006;127(6):1109-1122.
23. Bi P, Yue F, Sato Y, Wirbisky S, Liu W, Shan T, et al. Stage-specific effects of notch activation during skeletal myogenesis. Elife. 2016;5:e17355.
24. Nakao R, Inui R, Akamatsu Y, Goto M, Doi H, Matsuoka S. Illumina iSeq 100 and MiSeq exhibit similar performance in freshwater fish environmental DNA metabarcoding. Sci Rep. 2021;11(1):15763.
25. Bolyen E, Rideout JR, Dillon MR, Bokulich NA, Abnet CC, Al-Ghalith GA, et al. Reproducible, interactive, scalable and extensible microbiome data science using QIIME 2. Nat Biotechnol. 2019;37(8):852-857.
26. Yilmaz P, Parfrey LW, Yarza P, Gerken J, Pruesse E, Quast C, et al. The SILVA and "all-species Living Tree Project (LTP)" taxonomic frameworks. Nucleic Acids Res. 2014;42(D1):D643-D648.
27. Ruvinsky I, Meyuhas O. Ribosomal protein S6 phosphorylation: From protein synthesis to cell size. Trends Biochem Sci. 2006;31(6):342-348.
28. Fingar DC, Salama S, Tsou C, Harlow ED, Blenis J. Mammalian cell size is controlled by mTOR and its downstream targets S6K1 and 4EBP1/eIF4E. Genes Dev. 2002;16(12):1472-1487.
29. Ticinesi A, Lauretani F, Milani C, Nouvenne A, Tana C, Del Rio D, et al. Aging gut microbiota at the cross-road between nutrition, physical frailty, and sarcopenia: Is there a gut–muscle axis? Nutrients. 2017;9(12):1303.

30. White JP, Puppa MJ, Gao S, Sato S, Welle SL, Carson JA. Muscle mTORC1 suppression by IL-6 during cancer cachexia: A role for AMPK. Am J Physiol Endocrinol Metab. 2013;304(10):E1042-E1052.

31. Quinonez-Olivas CG, Salinas-Martinez R, Ortiz-Jimenez XA, Gamez-Trevino DG, Guajardo-Alvarez G, Gonzalez-Garcia B. Muscle mass measured using bioelectrical impedance analysis, calf circumference and grip strength in older adults. Medicina Universitaria. 2016;18(72):158-162.

32. Han DS, Chang KV, Li CM, Lin YH, Kao TW, Tsai KS, et al. Skeletal muscle mass adjusted by height correlated better with muscular functions than that adjusted by body weight in defining sarcopenia. Sci Rep. 2016;6(1):19457.

33. Evans WJ, Lexell J. Human aging, muscle mass, and fiber type composition. J Gerontol A Biol Sci Med Sci. 1995;50:11-16.

34. Verdijk LB, Snijders T, Beelen M, Savelberg HH, Meijer K, Kuipers H, et al. Characteristics of muscle fiber type are predictive of skeletal muscle mass and strength in elderly men. J Am Geriatr Soc. 2010;58(11):2069-2075.

35. Gao Z, Yin J, Zhang J, Ward RE, Martin RJ, Lefevre M, et al. Butyrate improves insulin sensitivity and increases energy expenditure in mice. Diabetes. 2009;58(7):1509-1517.

36. Pan JH, Kim JH, Kim HM, Lee ES, Shin DH, Kim S, et al. Acetic acid enhances endurance capacity of exercise-trained mice by increasing skeletal muscle oxidative properties. Biosci Biotechnol Biochem. 2015;79(9):1535-1541.

37. Moradi Y, Zehsaz F, Nourazar MA. Concurrent exercise training and *murf-1* and *atrogin-1 gene* expression in the vastus lateralis muscle of male wistar rats. Apunts Sports Med. 2020;55(205):21-27.

38. Kamada Y, Toyama S, Arai Y, Inoue H, Nakagawa S, Fujii Y, et al. Treadmill running prevents atrophy differently in fast-versus slow-twitch muscles in a rat model of rheumatoid arthritis. J Muscle Res Cell Motil. 2021;42(3-4):429-441.

39. Woo JH, Shin KO, Lee YH, Jang KS, Bae JY, Roh HT. Effects of treadmill exercise on skeletal muscle mTOR signaling pathway in high-fat diet-induced obese mice. J Phys Ther Sci. 2016;28(4):1260-1265.

40. Elfving B, Christensen T, Ratner C, Wienecke J, Klein AB. Transient activation of mTOR following forced treadmill exercise in rats. Synapse. 2013;67(9):620-625.

41. Bae JH, Seo DY, Lee SH, Shin C, Jamrasi P, Han J, et al. Effects of exercise on AKT/PGC1-α/FOXO3a pathway and muscle atrophy in cisplatin-administered rat skeletal muscle. Korean J Physiol Pharmacol. 2021;25(6):585.

42. Kim YA, Kim YS, Song W. Autophagic response to a single bout of moderate exercise in murine skeletal muscle. J Physiol Biochem. 2012;68:229-235.

43. Takegaki J, Ogasawara R, Tamura Y, Takagi R, Arihara Y, Tsutaki A, et al. Repeated bouts of resistance exercise with short recovery periods activates mTOR signaling, but not protein synthesis, in mouse skeletal muscle. Physiol Rep. 2017;5(22):e13515.

44. Zeng MY, Inohara N, Nunez G. Mechanisms of inflammation-driven bacterial dysbiosis in the gut. Mucosal Immunol. 2017;10(1):18-26.

45. Yamashiro K, Tanaka R, Urabe T, Ueno Y, Yamashiro Y, Nomoto K, et al. Gut dysbiosis is associated with metabolism and systemic inflammation in patients with ischemic stroke. PLoS One. 2017;12(2):e0171521.

46. Zhuang H, Cheng L, Wang Y, Zhang YK, Zhao MF, Liang GD, et al. Dysbiosis of the gut microbiome in lung cancer. Front Cell Infect Microbiol. 2019;9:112.

47. Luo J, Wang Z, Fan B, Wang L, Liu M, An Z, et al. A comparative study of the effects of different fucoidans on cefoperazone-induced gut microbiota disturbance and intestinal inflammation. Food Funct. 2021;12(19):9087-9097.

48. Han D, Li Z, Liu T, Yang N, Li Y, He J, et al. Prebiotics regulation of intestinal microbiota attenuates cognitive dysfunction induced by surgery stimulation in APP/PS1 mice. Aging Dis. 2020;11(5):1029.

49. Shang L, Liu H, Yu H, Chen M, Yang T, Zeng X, et al. Core altered microorganisms in colitis mouse model: A comprehensive time-point and fecal microbiota transplantation analysis. Antibiotics. 2021;10(6):643.

50. Pittayanon R, Lau JT, Yuan Y, Leontiadis GI, Tse F, Surette M, et al. Gut microbiota in patients with irritable bowel syndrome-A systematic review. Gastroenterology. 2019;157(1):97-108.

51. Poroyko VA, Carreras A, Khalyfa A, Khalyfa AA, Leone V, Peris E, et al. Chronic sleep disruption alters gut microbiota, induces systemic and adipose tissue inflammation and insulin resistance in mice. Sci Rep. 2016;6(1):35405.

52. Zhang J, Song L, Wang Y, Liu C, Zhang L, Zhu S, et al. Beneficial effect of butyrate-producing *Lachnospiraceae* on stress-induced visceral hypersensitivity in rats. J Gastroenterol Hepatol. 2019;34(8):1368-1376.

53. Li L, Zhong SJ, Hu SY, Cheng B, Qiu H, Hu ZX. Changes of gut microbiome composition and metabolites associated with hypertensive heart failure rats. BMC Microbiol. 2021;21(1):141.

54. Zeng H, Umar S, Rust B, Lazarova D, Bordonaro M. Secondary bile acids and short chain fatty acids in the colon: A focus on colonic microbiome, cell proliferation, inflammation, and cancer. Int J Mol Sci. 2019;20(5):1214.

55. Vinolo MA, Rodrigues HG, Nachbar RT, Curi R. Regulation of inflammation by short chain fatty acids. Nutrients. 2011;3(10):858-876.

56. Cherbut C, Aube AC, Blottiere HM, Galmiche JP. Effects of short-chain fatty acids on gastrointestinal motility. Scand J Gastroenterol Suppl. 1997;32(sup222):58-61.

57. Frampton J, Murphy KG, Frost G, Chambers ES. Short-chain fatty acids as potential regulators of skeletal muscle metabolism and function. Nat Metab. 2020;2(9):840-848.

58. Gao Z, Yin J, Zhang J, Ward RE, Martin RJ, Lefevre M, et al. Butyrate improves insulin sensitivity and increases energy expenditure in mice. Diabetes. 2009;58(7):1509-1517.

59. Walsh ME, Bhattacharya A, Sataranatarajan K, Qaisar R, Sloane L, Rahman MM, et al. The histone deacetylase inhibitor butyrate improves metabolism and reduces muscle atrophy during aging. Aging Cell. 2015;14(6):957-970.

60. Spina L, Cavallaro F, Fardowza NI, Lagoussis P, Bona D, Ciscato C, et al. Butyric acid: Pharmacological aspects and routes of administration. Digestive and Liver Disease Supplements. 2007;1(1):7-11.

61. Pant K, Saraya A, Venugopal SK. Oxidative stress plays a key role in butyrate-mediated autophagy *via* Akt/mTOR pathway in hepatoma cells. Chem Biol Interact. 2017;273:99-106.

62. Cao Y, Li Y, Han W, Jia X, Zhu P, Wei B, et al. Sodium butyrate ameliorates type 2 diabetes-related sarcopenia through il-33-independent ilc2s/il-13/stat3 signaling pathway. J Inflamm Res. 2023:343-358.

63. Evans MK, Savasi I, Heigenhauser GJ, Spriet LL. Effects of acetate infusion and hyperoxia on muscle substrate phosphorylation after onset of moderate exercise. Am J Physiol Endocrinol Metab. 2001;281(6):E1144-E1450.

64. Okamoto T, Morino K, Ugi S, Nakagawa F, Lemecha M, Ida S, et al. Microbiome potentiates endurance exercise through intestinal acetate production. Am J Physiol Endocrinol Metab. 2019;316(5):E956-E966.

65. Boulange CL, Neves AL, Chilloux J, Nicholson JK, Dumas ME. Impact of the gut microbiota on inflammation, obesity, and metabolic disease. Genome Med. 2016;8(1):1-2.

66. Cristofori F, Dargenio VN, Dargenio C, Miniello VL, Barone M, Francavilla R. Anti-inflammatory and immunomodulatory effects of probiotics in gut inflammation: A door to the body. Front Immunol. 2021;12:578386.

67. Glorieux G, Gryp T, Perna A. Gut-derived metabolites and their role in immune dysfunction in chronic kidney disease. Toxins. 2020;12(4):245.